Separation of applied stress and temperature effects on ultrasonic guided wave phase

Oleg Lobkis, Chris Larsen, and Richard Roth II

Citation: AIP Conference Proceedings **1650**, 211 (2015); doi: 10.1063/1.4914612
View online: http://dx.doi.org/10.1063/1.4914612
View Table of Contents: http://scitation.aip.org/content/aip/proceeding/aipcp/1650?ver=pdfcov
Published by the AIP Publishing

Articles you may be interested in

An ultrasonic guided wave method to estimate applied biaxial loads
AIP Conf. Proc. **1430**, 1567 (2012); 10.1063/1.4716401

COMPARISON OF THE EFFECTS OF APPLIED LOADS AND TEMPERATURE VARIATIONS ON GUIDED WAVE PROPAGATION
AIP Conf. Proc. **1335**, 175 (2011); 10.1063/1.3591854

Nonlinear resonance interaction of ultrasonic waves under applied stress
J. Appl. Phys. **56**, 235 (1984); 10.1063/1.333759

Effect of Multimode Guided Wave Propagation on Ultrasonic Phase Velocity Measurements: Problem and Remedy
J. Acoust. Soc. Am. **45**, 341 (1969); 10.1121/1.1972261

Effect of Statically Applied Stresses on the Velocity of Propagation of Ultrasonic Waves
J. Appl. Phys. **29**, 1736 (1958); 10.1063/1.1723035

This article is copyrighted as indicated in the article. Reuse of AIP content is subject to the terms at: http://scitation.aip.org/termsconditions. Downloaded to IP: 207.250.97.74 On: Wed, 01 Apr 2015 13:40:31

Separation of Applied Stress and Temperature Effects on Ultrasonic Guided Wave Phase

Oleg Lobkis[a)], Chris Larsen, and Richard Roth II

Etegent Technologies Ltd
5050 Section Ave., Suite 110
Cincinnati, OH, USA 45212

[a)]Corresponding author: oleg.lobkis@etegent.com

Abstract. An investigation was conducted into the simultaneous effects of applied uniaxial stress and temperature change on the compressional guided wave in a cylindrical waveguide. Due to stress directional anisotropy and temperature isotropy these two effects exhibit differing frequency dependence. This allows for the influences of stress and temperature on the ultrasonic wave properties to be separated. Separation of these effects could be used to enable an accurate measurement of applied stress in fluctuating temperature environments.

INTRODUCTION

Both temperature and applied stress have an effect on the properties of ultrasonic waves in a material. This allows ultrasonic data to be used for measurement of external temperature and applied stress [1]. Propagating waves are inherently dispersive in cylindrical waveguides; both temperature changes and applied stress alter the dispersive characteristics, producing changes with a complicated dependence on frequency. Changes in the dispersive characteristics are caused by two underlying physical phenomena. First is geometric changes, including axial and lateral thermal expansion as well as strain. Second are changes in the elastic properties of the waveguide material, again influenced both by temperature and stress (via acoustoelasticity). As a result the ultrasonic wave parameters (phase, velocity, time of flight) depend on external temperature and applied stress.

THEORY

Consider the general case of guided wave propagation in the presence of both an applied force ΔF and a temperature change ΔT (Fig. 1). These changes in the temperature and force produce changes in both the geometry of the waveguide and its elastic properties. A number of specific geometric changes can be identified:

1. The length of the waveguide changes due to temperature by $\Delta l_T = \alpha \Delta T l_0$, where α is the linear thermal expansion coefficient and l_0 is initial waveguide length.
2. The radius of the waveguide changes due to temperature by $\Delta r_T = \alpha \Delta T r_0$, where r_0 is the initial waveguide radius.
3. The length of the waveguide changes due to force by $\Delta l_\varepsilon = \Delta \varepsilon l_0$, where $\Delta \varepsilon$ is the strain in waveguide due to applied force (force, stress=force/area and strain are proportional to each other through Hook's law and in further analysis we will use strain as the independent variable).
4. The radius of the waveguide changes due to force (via the Poisson effect) by $\Delta r_\varepsilon = -\nu \, \Delta \varepsilon r_0$, where ν is the Poisson ratio.

41st Annual Review of Progress in Quantitative Nondestructive Evaluation
AIP Conf. Proc. 1650, 211-220 (2015); doi: 10.1063/1.4914612
© 2015 AIP Publishing LLC 978-0-7354-1292-7/$30.00

This article is copyrighted as indicated in the article. Reuse of AIP content is subject to the terms at: http://scitation.aip.org/termsconditions. Downloaded to IP: 207.250.97.74 On: Wed, 01 Apr 2015 13:40:31

In general, the guided wave's phase velocity V at some frequency f will depend on temperature, strain, and the wire radius as $V(T,\varepsilon,r)$.

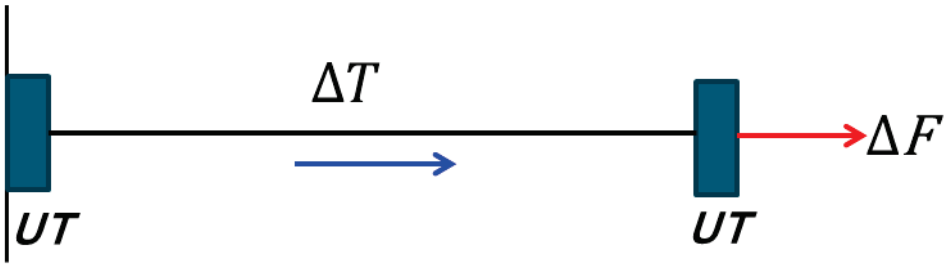

FIGURE 1. Waveguide between two ultrasonic transducers (UT) under temperature change ΔT and applied force ΔF.

For continuous wave (CW) excitation the signal dependence on time t is $\sin(2\pi ft-\varphi)$. The instantaneous propagating wave phase $\varphi = 2\pi f l(T,\varepsilon)/V(T,\varepsilon,r)$ itself is time-varying, dependent on both waveguide geometry and the phase velocity, which are in turn functions of the external conditions. These effects can be approximated in a region near the initial conditions by using a series expansion and limiting to the linear terms, $l(T,\varepsilon) = l_0 + \Delta l_T + \Delta l_\varepsilon$ and $V(T,\varepsilon,r) = V_0 + \frac{\partial V}{\partial T}\Delta T + \frac{\partial V}{\partial \varepsilon}\Delta\varepsilon + \frac{\partial V}{\partial r}(\Delta r_T + \Delta r_\varepsilon)$. These terms may then be inserted into the phase expression, yielding

$$\varphi = \frac{2\pi f l}{V} = \frac{2\pi f (l_0 + \Delta l_T + \Delta l_\varepsilon)}{V_0 + \frac{\partial V}{\partial T}\Delta T + \frac{\partial V}{\partial \varepsilon}\Delta\varepsilon + \frac{\partial V}{\partial r}(\Delta r_T + \Delta r_\varepsilon)} = \frac{\varphi_0(1+\alpha\Delta T + \Delta\varepsilon)}{1+\beta\Delta T + \gamma\Delta\varepsilon + \delta(\alpha\Delta T - \nu\Delta\varepsilon)} \tag{1}$$

The rightmost version of the equation defines new symbols for the velocity gradients with respect to temperature, strain, and radius, $\beta = \frac{1}{V_0}\frac{\partial V}{\partial T}$, $\gamma = \frac{1}{V_0}\frac{\partial V}{\partial \varepsilon}$, and $\delta = \frac{r_0}{V_0}\frac{\partial V}{\partial r}$. Further simplification shows the dependence of the relative phase change on temperature and strain to be linear:

$$\frac{\Delta\varphi}{\varphi_0} \approx (\alpha - \alpha\delta - \beta)\Delta T + (1 + \delta\nu - \gamma)\Delta\varepsilon = s_T(f)\Delta T + s_\varepsilon(f)\Delta\varepsilon \tag{2}$$

Here φ_0 is the phase at the initial temperature and stress. The slopes with respect to temperature, $s_T(f) = \alpha - \alpha\delta - \beta$, and strain, $s_\varepsilon(f) = 1 + \delta\nu - \gamma$, are frequency dependent; analysis of these dependencies is the focus of the remainder of this paper. This approach could be used to investigate any guided modes (e.g. torsional or flexural), but only the longitudinal L_{01} mode will be further explored here.

Temperature Slope

The temperature dependence of the L_{01} guided wave's phase velocity can be calculated given the temperature dependence of the bulk velocities. In general the elastic moduli and the bulk velocities in materials decrease with temperature [2] (that is, materials become more compliant). For example, in mild steel the relative temperature gradients of the longitudinal and shear bulk velocities are $\beta_l = \frac{1}{V_l}\frac{\partial V_l}{\partial T} \approx -1.5\cdot 10^{-4}\ 1/℃$ and $\beta_s = \frac{1}{V_s}\frac{\partial V_s}{\partial T} \approx -2.2\cdot 10^{-4}\ 1/℃$ [2]. These relative temperature gradients for bulk waves can be incorporated into the relative temperature gradient calculation for the guided wave. First the frequency dependence of the guided wave's phase velocity $V(T)$ is calculated from the Pochhammer rod equation [3] for some temperature T, using the material elastic parameters $V_{l,s}(T)$. Then the same equation is employed for a new temperature $T+\Delta T$ and new material parameters $V_{l,s}(T+\Delta T) \approx V_{l,s}(T)(1+\beta_{l,s}\Delta T)$ to get the phase velocity $V(T+\Delta T)$. Then the frequency dependence of the

This article is copyrighted as indicated in the article. Reuse of AIP content is subject to the terms at: http://scitation.aip.org/termsconditions. Downloaded to IP: 207.250.97.74 On: Wed, 01 Apr 2015 13:40:31

relative temperature gradient for the guided wave's phase velocity is computed numerically as $= \frac{1}{V}\frac{\partial V}{\partial T} \approx \frac{V(T+\Delta T)-V(T)}{V(T)\Delta T}$. The result of this numerical calculation versus frequency is presented in Fig. 2a for a steel rod (room temperature bulk velocities are $V_l = 5.96\, mm/\mu s$ and $V_s = 3.26\, mm/\mu s$). It should be noted that the shape of the curve for a cylindrical waveguide is similar to the shape for S_0 Lamb wave in a plate [4].

While the frequency dependence of the temperature gradient $\beta(f)$ can, in general, only be calculated numerically, it is possible to analytically investigate the limiting high and low frequency cases. The rod velocity V_r (that is, the low frequency limit) has an explicit dependence on the bulk velocities (left expression in Eq. 3). Taking the derivative with respect to temperature of both sides of the equation yields $\beta_r = \frac{1}{V_r}\frac{\partial V_r}{\partial T}$, the low frequency limit of the rod velocity's temperature gradient. This is a function of the temperature coefficients of the bulk velocities $\beta_{l,s}$ and the Poisson ratio ν.

$$V_r = V_s\sqrt{\frac{3V_l^2 - 4V_s^2}{V_l^2 - V_s^2}}; \quad \beta_r = \beta_s + (\beta_l - \beta_s)\frac{(1-\nu)(1-2\nu)}{(1+\nu)} \tag{3}$$

At the high frequency limit the L_{01} guided wave behavior approaches that of a Rayleigh wave, with wave velocity V_R (left expression in Eq. 4). Again taking the derivative with respect to temperature yields $\beta_R = \frac{1}{V_R}\frac{\partial V_R}{\partial T}$, the high frequency limit of the phase velocity's temperature gradient. This is again an explicit function of the coefficients $\beta_{l,s}$ and ν.

$$V_R \approx V_s\frac{0.87+1.12\nu}{1+\nu}; \quad \beta_R \approx \beta_s + (\beta_l - \beta_s)\frac{(1-\nu)(1-2\nu)}{2(0.87+1.12\nu)(1+\nu)} \tag{4}$$

For a steel rod ($\nu \approx 0.29$) the limits are $\beta_r \approx 0.77\beta_s + 0.23\beta_l$ and $\beta_R \approx 0.91\beta_s + 0.09\beta_l$. This shows that contribution of the shear wave's temperature dependence is dominant for both the rod and the Rayleigh wave velocities. Using the temperature gradients of the bulk velocities presented in [2] these values can be calculated as $\beta_r \approx -2.0 \cdot 10^{-4}$ 1/°C and $\beta_R \approx -2.1 \cdot 10^{-4}$ 1/°C.

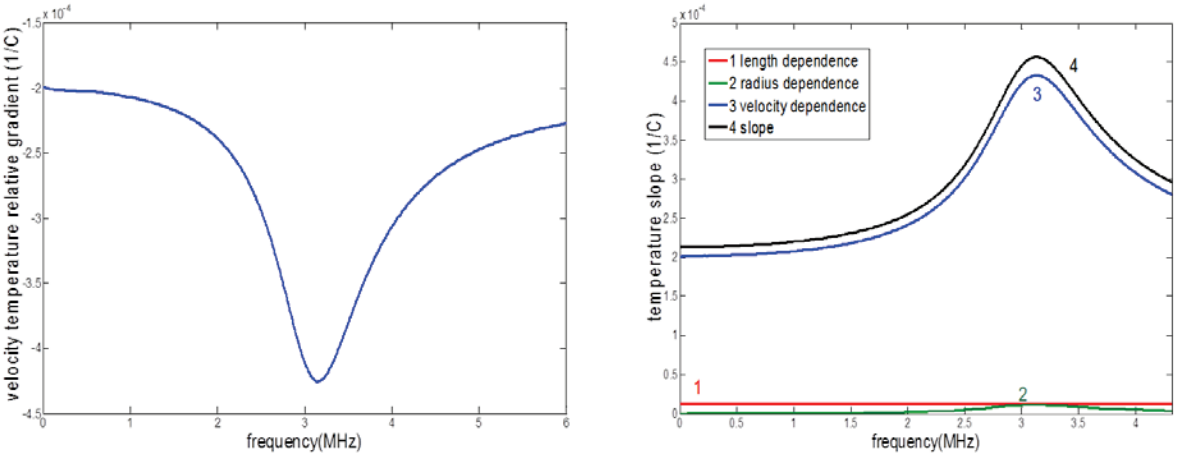

(a) (b)

FIGURE 2. The phase velocity's temperature gradient β (a) and temperature slope s_T and its components $(\alpha, -\alpha\delta, -\beta)$ (b) versus frequency for a 1 mm diameter steel rod. The bulk velocities temperature gradients are $\beta_l = -1.5 \cdot 10^{-4}$ 1/°C and $\beta_s = -2.2 \cdot 10^{-4}$ 1/°C.

Numerical evaluation of the phase velocity's temperature gradient for a 1 mm diameter steel rod is shown in Fig. 2a, where this limit-bounded behavior is evident. Figure 2b shows the temperature slope and its components. The full numerical evaluation in Fig. 2a shows that the L_{01} guided wave's phase velocity is most sensitive to temperature

This article is copyrighted as indicated in the article. Reuse of AIP content is subject to the terms at: http://scitation.aip.org/termsconditions. Downloaded to IP: 207.250.97.74 On: Wed, 01 Apr 2015 13:40:31

changes in the dispersive region, where the absolute value of the temperature gradient is about twice what it is in the low and high frequency regimes, with $max|\beta| \approx 4.3 \cdot 10^{-4}\ 1/℃$. The numerical calculations are in good agreement with the analytical high and low frequency expressions.

It's also possible to compare the change in elastic properties due to the effects of temperature and thermal expansion. The linear thermal expansion coefficient α is of much smaller magnitude than the coefficient β, with $\alpha = 1.2 \cdot 10^{-5}\ 1/℃$ for steel. These values can be used to analyze the temperature slope, $s_T = \alpha - \alpha\delta - \beta$, as a function of frequency. The net temperature slope must be positive, since $\alpha > 0$, $\alpha\delta < 0$, and $\beta < 0$. Figure 2b shows the temperature slope s_T versus frequency for the longitudinal L_{01} mode in a 1 mm diameter steel rod. The three components of this quantity ($-\beta$, α, and $-\alpha\delta$) are also plotted for reference. It is obvious from the graph that s_T is determined mostly by the phase velocity's dependence on temperature, $-\beta$; the other two terms contribute less than 10% to the overall temperature slope.

Strain Slope

Calculation of the strain slope $s_\varepsilon = 1 + \delta\nu - \gamma$ is more complicated than that of the temperature slope. Even if the length and radius variations due to stress (i.e. the first two terms of the s_ε equation) are straightforward the dependence of the elastic properties on stress (i.e. the acoustoelastic coefficient γ) still requires a more sophisticated analysis. For example, the change in the elastic properties is isotropic with temperature variation. This means that the longitudinal and shear velocities vary in the same manner in both the axial and lateral directions of the waveguide, and thus the originally isotropic waveguide remains isotropic at any temperature. On the other hand, the change in the elastic properties is directionally dependent on the stress. An originally isotropic waveguide can become anisotropic in the presence of stress.

Consider a uniaxial stress along the waveguide axis (i.e. axis 3 in Fig. 3). Under uniaxial stress in direction 3 due to cylindrical symmetry the waveguide will be transversely isotropic, with physical properties that are isotropic in the normal plane 1-2. In planes 1-3 and 2-3 an originally isotropic material will transform to one that is weakly anisotropic, due to the stress.

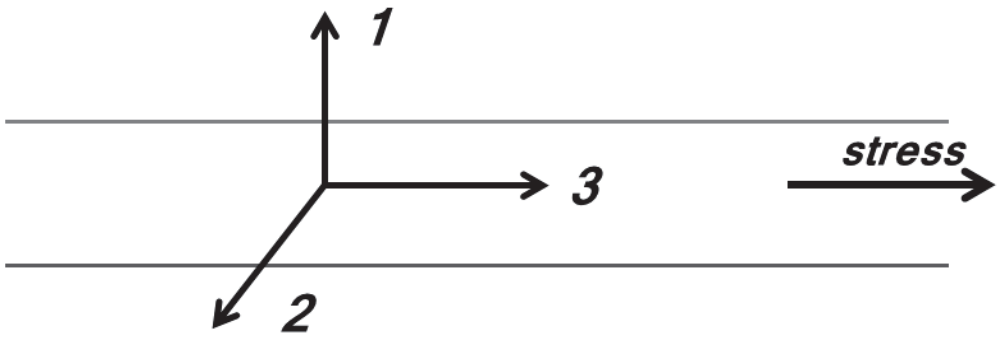

FIGURE 3. Waveguide under uniaxial stress (1-2 is the plane of symmetry, 3 is the axis of symmetry).

The stiffness matrix for transversely isotropic material is described by five independent elastic constants. Two constants in the isotropic plane 1-2 are C_{11} and C_{66}, and three constants in the anisotropic plane 1-3 are C_{33}, C_{13}, and C_{55}. Under applied stress in the direction 3 the appropriate strain components are $(-\nu\varepsilon, -\nu\varepsilon, \varepsilon)$ and the elastic constants transform to [5]:

in plane 1-2

$$C_{11} = \lambda + 2\mu + \left[2l + \lambda - \nu\left(4l + 4m + 4\lambda + 6\mu\right)\right]\varepsilon$$
$$C_{66} = \mu + \left[m + n/2 + \lambda - \nu\left(2m + 2\lambda + 4\mu\right)\right]\varepsilon \qquad (5)$$

This article is copyrighted as indicated in the article. Reuse of AIP content is subject to the terms at: http://scitation.aip.org/termsconditions. Downloaded to IP: 207.250.97.74 On: Wed, 01 Apr 2015 13:40:31

$$C_{33} = \lambda + 2\mu + \left[2l + 4m + 3\lambda + 6\mu - \nu\left(4l + 2\lambda\right)\right]\varepsilon$$

in plane 1-3 $$C_{13} = \lambda + \left[2l + \lambda - \nu\left(4l - 2m + n + \lambda\right)\right]\varepsilon \qquad (6)$$

$$C_{55} = \mu + \left[m + \lambda + 2\mu - \nu\left(2m - n/2 + 2\lambda + 4\mu\right)\right]\varepsilon$$

where λ and μ are the Lame constants or the second order elastic constants (SOECs) and l, m, and n are the Murnaghan constants or the third order elastic constants (TOECs). The linear and nonlinear elastic constants are presented in Table 1 for different types of steel. Note that the SOECs remain similar to each other across the listed materials, while the TOECs vary greatly for different types of steel [6].

TABLE 1. The second and third order elastic constants (SOECs λ and μ, and TOECs l, m, and n) for different types of steel.

Steel Type	$\lambda\,(GPa)$	$\mu\,(GPa)$	ν	$l\,(GPa)$	$m\,(GPa)$	$n\,(GPa)$
Rail Steel	115.8	79.9	0.296	−248	−623	−714
E 295	110	83	0.285	−251	−519	−656
22NiMOCr37	109.1	81.9	0.286	−196	−520	−657
E 42	110.4	81.4	0.288	−48	−501	−640
Mild Steel	113	80.9	0.291	−197	−892	−1010
Low Carbon	110	82.1	0.286	−850	−518	−1781

The phase velocity's strain gradient, γ, can be calculated in the same way as the temperature gradient β. First the phase velocity is calculated for an isotropic waveguide $V(\varepsilon = 0)$ using the Pochhammer rod equation [3], then new elastic constants (eq. 5 and 6) are obtained for some small strain ε. The phase velocity $V(\varepsilon)$ for the L_{01} mode is then calculated for a transversely isotropic waveguide [7]. The phase velocity's strain gradient (acoustoelastic coefficient) is then the normalized difference of these two phase velocities, or $\gamma = \frac{1}{V}\frac{\partial V}{\partial \varepsilon} \approx \frac{V(\varepsilon) - V(\varepsilon=0)}{V(\varepsilon=0)\varepsilon}$, and can be estimated at any frequency. Figure 4a presents the dependence of the acoustoelastic coefficient γ versus frequency for a 1 mm diameter steel rod.

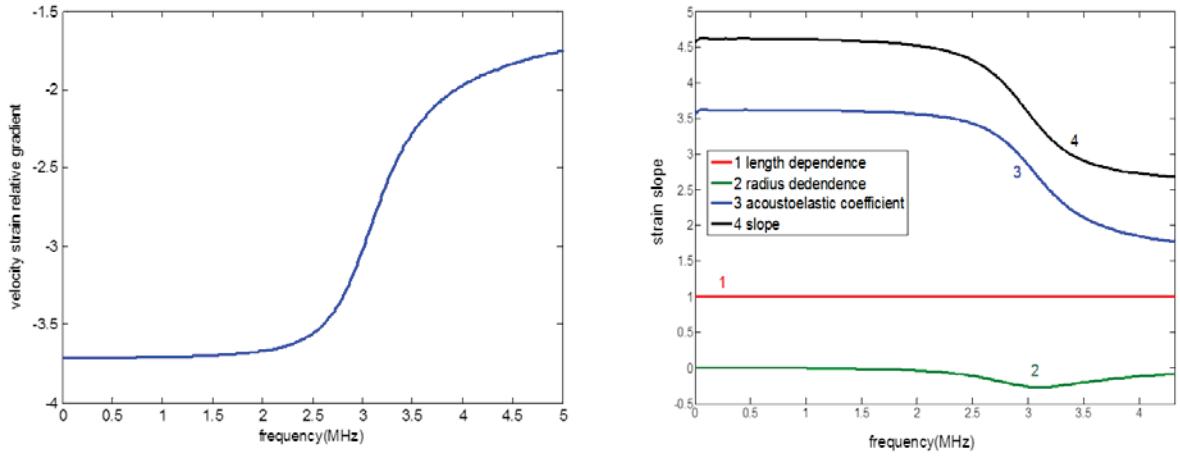

(a) (b)

FIGURE 4. The phase velocity's relative strain gradient γ (i.e. acoustoelastic coefficient) (a) and the strain slope s_ε and its components $(1, -\nu\delta, -\gamma)$ versus frequency for a 1 mm diameter steel rod.

One can see that the shape of this curve is different from that of the temperature gradient β. The coefficient γ is negative and the velocity decreases with increasing frequency. Once again the low and high frequency limiting cases can be calculated analytically and compared with the numerical results. At low frequency the rod velocity V_r has an explicit dependence on the elastic constants (the left dependence in Eq.7) [7]. Substituting the expressions from equations 5 and 6 for the elastic constants and taking their derivatives with respect to the strain ε gives an expression for the rod velocity strain gradient γ_r

This article is copyrighted as indicated in the article. Reuse of AIP content is subject to the terms at: http://scitation.aip.org/termsconditions. Downloaded to IP: 207.250.97.74 On: Wed, 01 Apr 2015 13:40:31

$$\rho V_r^2 = C_{33} - \frac{C_{13}^2}{C_{11} - C_{66}}; \quad \gamma_r = \frac{1}{V_r}\frac{dV_r}{d\varepsilon} = \frac{3}{2} + \frac{1}{E}\left[(1-2\nu)^3 l + 2(1+\nu)^2(1-2\nu)m + 3\nu^2 n\right] \tag{7}$$

which depends on the Young's modulus E, the Poisson ratio ν, and the TOECs l, m, and n. For steel ($E \approx 210\ GPa$, $\nu \approx 0.3$) the acoustoeleastic coefficient for the rod velocity is equal to $\gamma_r \approx 1.5 + 6.44 \cdot 10^{-3}(0.047l + m + 0.2n)$. This expression shows that at low frequency the strain gradient depends mostly on one of the TOECs, m. Thus, choosing a steel type with the highest sensitivity to the applied stress is almost equivalent to finding the material with the largest (and negative) TOEC m. At high frequencies, when the L_{01} guided wave approaches a Rayleigh form, only an implicit form of the Rayleigh wave velocity V_R for a transversely isotropic medium is available , as shown in equation 8 [8]. Taking the strain derivatives of both sides of it gives an implicit equation for high frequency limit acoustoelastic coefficient $\gamma_R = \frac{1}{V_R}\frac{\partial V_R}{\partial \varepsilon}$.

$$\eta = (C - \eta)\sqrt{\frac{C_{11}(C_{55} - \eta)}{C_{55}(C_{33} - \eta)}}; \quad \eta = \rho V_R^2; \quad C = C_{33} - \frac{C_{13}^2}{C_{11}} \tag{8}$$

The strain slope dependence $s_\varepsilon = 1 + \nu\delta - \gamma$ versus frequency is presented in Fig. 4b for a 1 mm diameter steel rod, along with separate plots with the three components (1, $\nu\delta$, and $-\gamma$). It is obvious that the slope is positive because $\delta < 0$, $|\delta| < 1$, $\nu < 1$, $1 + \nu\delta > 0$, and $\gamma < 0$. For this example about 77% of the contribution come from acoustoelasticity, but this value strongly depends on the steel type.

Comparison of Temperature and Strain Effects

The relative magnitude of the temperature and strain effects and be readily compared by examining Fig. 3a and Fig. 4a, where the peak magnitudes can be seen to be as $\max(s_T) \approx 4.5 \cdot 10^{-4}$ and $\max(s_\varepsilon) \approx 4.5$. This means that 10^{-4} strain is equivalent to 1℃ temperature change for steel with these temperature and acoustoelastic material properties. It is clear that measuring strain with high accuracy requires either a high degree of temperature stability or an accurate temperature compensation technique.

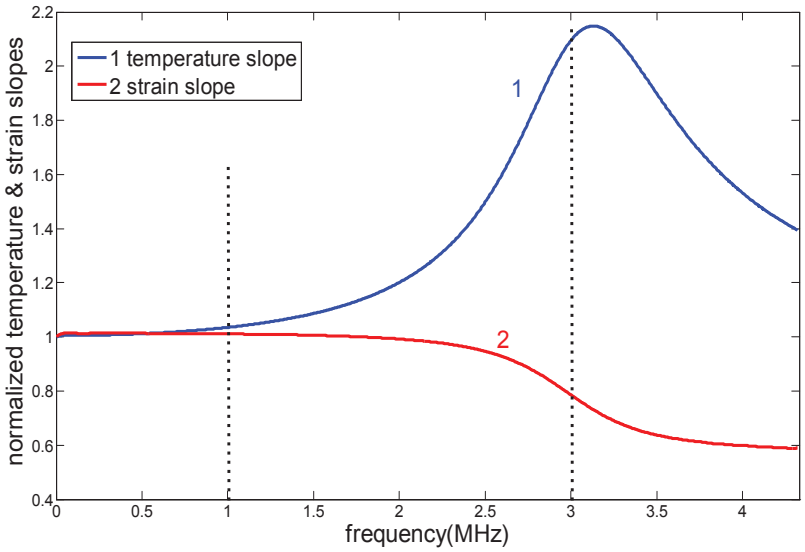

FIGURE 5. The normalized temperature s_T and strain s_ε slopes versus frequency for a 1 mm diameter steel rod.

The different behaviors with frequency of the temperature s_T and the strain s_ε slopes can be used to separate the effects of environmental temperature and applied stress. Figure 5 presents the temperature and strain normalized

This article is copyrighted as indicated in the article. Reuse of AIP content is subject to the terms at: http://scitation.aip.org/termsconditions. Downloaded to IP: 207.250.97.74 On: Wed, 01 Apr 2015 13:40:31

slopes together. Measuring the phase gradient at two frequencies (for example, 1 MHz and 3 MHz in Fig. 5) one obtains two independent instances of equation 2 for the relative phase change. If s_T and s_ε are known functions of frequency this system of equations can be used to solve for the temperature ΔT and the strain $\Delta\varepsilon$.

EXPERIMENTAL RESULTS

Figure 6 presents the experimental setup used to verify the theory presented above. An ultrasonic wave is excited and sensed in a steel waveguide using a pair of ultrasonic transducers (UT). The design of the waveguide allows for the application of stress with the applied force measured by an S-shaped load cell. A portion of the waveguide is enclosed in a heater, allowing for temperature control. It should be noted that due to the complex temperature profile produced by the heater the average temperature changes cannot be measured directly; rather, the ultrasonic data is the sole estimator of the average temperature. A continuously pulsing wave is excited at the transmitting transducer using an arbitrary function generator. By modifying the duty cycle it is possible to simultaneously transmit several frequencies within the transducer's bandwidth. In the experiment detailed here an 80% (positive) duty cycle pulse wave was excited at four harmonics with relative amplitudes of 0.749, 0.606, 0.404, and 0.187. The frequency of the first harmonic can be modified to excite a second set of frequencies in a range convenient for analysis. The temperature inside the heater is allowed to drop from 50 ℃ to 25 ℃ for each measurement. The initial test varied only the temperature, allowing the phase change to be used as a direct temperature measurement. Test results are shown in Fig. 7a for a 1 mm diameter steel rod evaluated at frequencies of 0.72, 1.44, 2.16, and 2.88 MHz. The first frequency is then changed to about 0.74 MHz and the temperature dependence test was repeated.

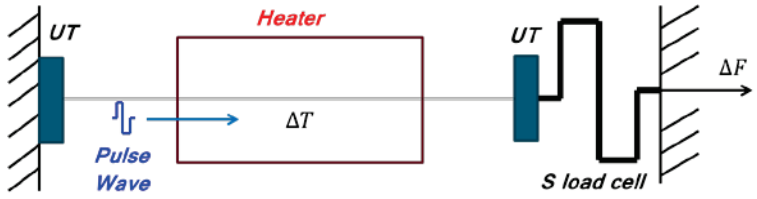

FIGURE 6. Experimental setup for testing the waveguide under temperature change and applied stress.

The frequency range was restricted by the first cut-off frequency to avoid the excitation of high order longitudinal guided wave modes. Figure 7b presents both the experimental and the theoretical normalized behavior of the temperature slope s_T versus frequency. In the frequency interval tested an approximately correct rise in the temperature gradient with frequency was observed.

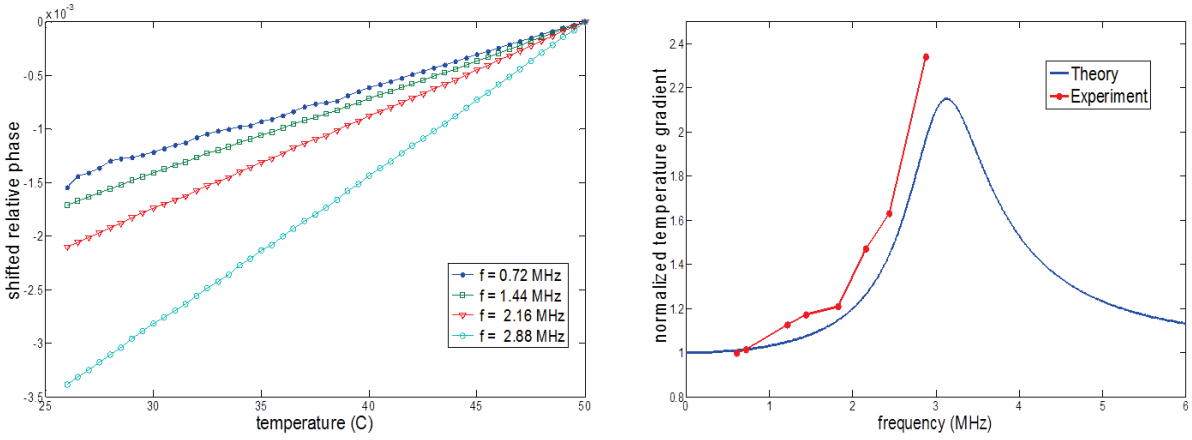

(a) (b)

FIGURE 7. Relative phase dependence versus temperature for different frequencies (a), and the normalized temperature slopes versus frequency, experiment and theory (b) for the 1mm diameter steel rod.

This article is copyrighted as indicated in the article. Reuse of AIP content is subject to the terms at: http://scitation.aip.org/termsconditions. Downloaded to IP: 207.250.97.74 On: Wed, 01 Apr 2015 13:40:31

To find the strain slope the ultrasonic phase change in the waveguide was measured under applied stress at constant temperature. Music steel (a high-carbon or spring steel) wire with 0.36 mm diameter was used for this test. It's important to note that initial tests on this material show a weaker dependence on the acoustoelastic effect than the steel rods that have been used in past tests – the music steel wire shows a strain slope of about 1.2 at low frequency, as compared to an expected 4.5 for another steel (see Fig. 4). Figure 8a shows the CW phase at several frequencies. It is evident that the phase change with force decreases at higher frequencies. At a frequency of 6.46 MHz the strain slope is close to zero, which means that the ultrasonic wave is insensitive to the applied stress. The broader frequency dependence of the strain slope is presented in Fig. 8b. In spite of the low sensitivity of music steel to the applied stress the shape of the curve agrees well with the theoretical data presented in from Fig. 4b.

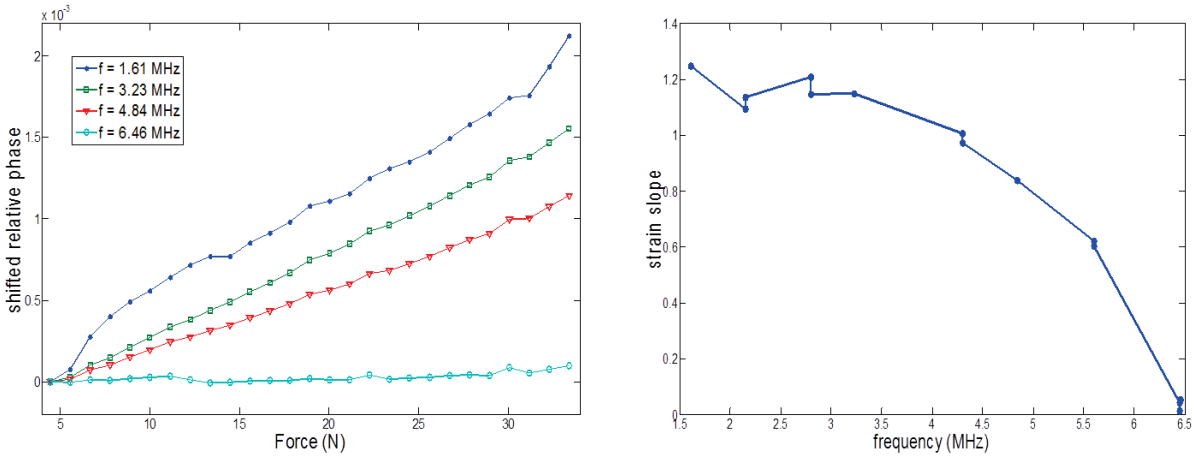

(a) (b)

FIGURE 8. Relative phase dependence versus applied force for different frequencies (a), and the measured strain slope s_ε versus frequency (b) for the 0.36 mm diameter music steel wire.

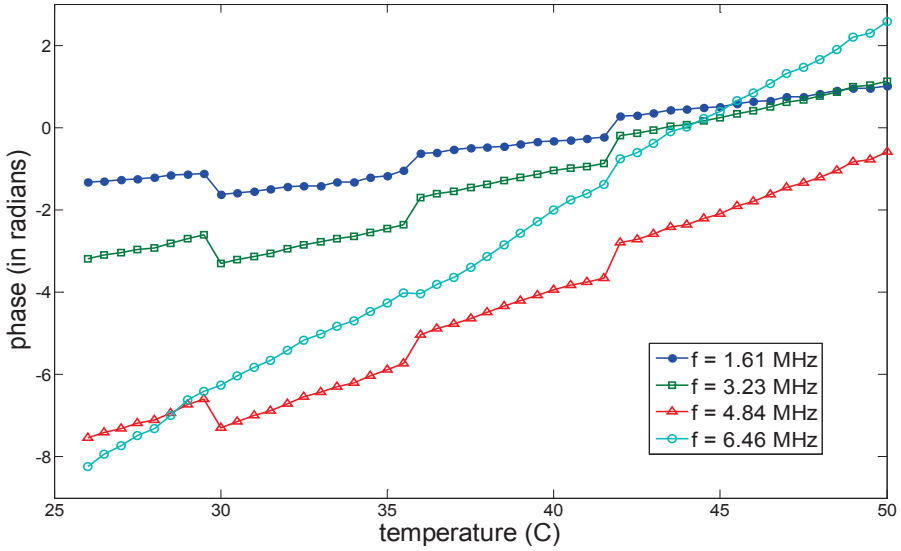

FIGURE 9. The phase change versus temperature and applied force at 1.61, 3.23, 4.84, and 6.46 MHz for 0.36 mm diameter music steel wire.

As an example of the separation of temperature and applied force, guided wave propagation in the 0.36 mm diameter wire was investigated under simultaneous changes in temperature and applied force. To prepare the experiment the wire was pre-stressed and the temperature in the heater was raised. During the cool down of the heater

This article is copyrighted as indicated in the article. Reuse of AIP content is subject to the terms at: http://scitation.aip.org/termsconditions. Downloaded to IP: 207.250.97.74 On: Wed, 01 Apr 2015 13:40:31

(at temperatures of approximately 43, 36, and 30 ℃) an external force was applied to the wire both in positive (extension) and negative (compression) directions three times.

Signals were acquired by the oscilloscope at approximately every 1℃ during cool down and were processed to obtain the phase of the guided wave at each frequency. Figure 9 shows the phases plotted as a function of temperature at each frequency tested. The "jumps" that are evident in the data are caused by the changes in the applied force. The relative phase change $\Delta\varphi_n/\varphi_n$ for the four harmonics is a function of the changes in the temperature ΔT and the force ΔF, as well as the 2x4 temperature-force slopes matrix s.

$$\begin{Bmatrix} \Delta\varphi_n \\ \varphi_n \end{Bmatrix} = s \begin{Bmatrix} \Delta T \\ \Delta F \end{Bmatrix}; \qquad \begin{Bmatrix} \Delta T \\ \Delta F \end{Bmatrix} = s^{-1} \begin{Bmatrix} \Delta\varphi_n \\ \varphi_n \end{Bmatrix}, \quad n = 1,2,3,4 \tag{9}$$

Due to the different dependence on temperature and force for each frequency the system of equations can be solved and the temperature and force changes can be extracted. Beginning at an initial condition of $T = 50$℃ and $F = 0\ lbs$ the system of equations is solved at each acquisition step to obtain the changes in temperature and force.

Figure 10a compares the temperature recovered via this method with the directly measured temperature in the heater; the agreement of the measurements is quite good. The small jumps in the measured temperature at the key temperatures where force was varied (43, 36, and 30 ℃) show reasonable accuracy in the temperature reconstruction. Similarly, the recovered and directly measured external forces are shown in Fig. 10b. Discrepancies of a few percent between the directly measured and recovered values show the limits of the accuracy of this method. However, the applied force values extracted from the ultrasonic data are relatively stable (horizontal lines) for successive measurements at the same external force. This shows that the force measurements are at least fairly repeatable in spite of the constantly changing temperatures.

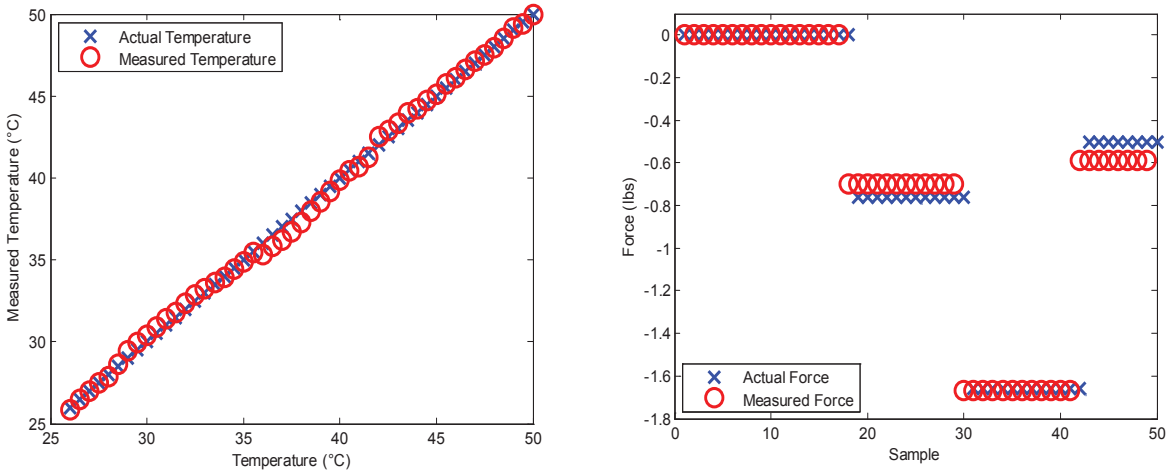

(a) (b)

FIGURE 10. Separation of the temperature and applied force changes.

CONCLUSION

An analysis of the effects of simultaneously changing temperature and applied stress on the propagation of a guided wave was conducted. It was shown that the effect of changing temperature can mask the effect of stress, and vice versa. The temperature and stress dependencies on frequency were shown to be different, due the directionality of the stress and the isotropy of the temperature changes. These differences allow for the separation of the two effects, and for the use of ultrasonic data to measure an applied stress in environments where the temperature fluctuates.

This article is copyrighted as indicated in the article. Reuse of AIP content is subject to the terms at: http://scitation.aip.org/termsconditions. Downloaded to IP: 207.250.97.74 On: Wed, 01 Apr 2015 13:40:31

ACKNOWLEDGMENTS

This work is dedicated to the late Chris Larsen, whose contributions are innumerable, and was sponsored by NAVY under contract N68335-11-C-0385.

REFERENCES

1. L. C. Lynnworth, *Ultrasonic Measurements for Process Control* (Academic Press, San Diego, 1989).
2. C. B. Scruby and B. C. Moss, "Non-contact ultrasonic measurements on steel at elevated temperatures", NDT&E International **26**, 177-188 (1993).
3. J. Qu and L. Jacobs, "Cylindrical Waveguides and Their Applications in Ultrasonic Applications", in *Ultrasonic NDE for Engineering and Biological Material Characterization*, edited by T. Kundu (CRC Press, Boca Raton, FL, 2003), pp. 311–362.
4. J. C. Dodson and D. J. Inman, "Thermal sensitivity of Lamb waves for structural health monitoring applications", *Ultrasonics* **53**, 677-685 (2013).
5. Y.-H. Pao and U. Gamer, "Acoustoelastic waves in orthotropic media", *J. Acoust. Soc. Amer.*, **77**, 806-812 (1985).
6. V. Hauk, *Structural and Residual Stress Analysis by Nondestructive Methods* (Elsevier, Amsterdam, 1997).
7. P.B. Nagy, "Longitudinal guided wave propagation in a transversely isotropic rod immersed in fluid", *J. Acoust. Soc. Amer.*, **98**, 454-457 (1995).
8. D. Royer and E. Dieulesaint, "Rayleigh wave velocity and displacement in orthorhombic, tetragonal, hexagonal and cubic crystals", *J. Acoust. Soc. Amer.*, **76**, 1438-1444 (1984).

This article is copyrighted as indicated in the article. Reuse of AIP content is subject to the terms at: http://scitation.aip.org/termsconditions. Downloaded to IP: 207.250.97.74 On: Wed, 01 Apr 2015 13:40:31